



Numerical Analysis of Ship Motion of Crew Boat with Variations of Wave Period on Ship Operational Speed

Amalia Ika Wulandari¹, I Ketut Aria Pria Utama^{1,*}, Afifah Rofidayanti¹, Dominic Hudson²

¹ Department of Naval Architecture, Faculty of Marine Technology, Institut Teknologi Sepuluh Nopember, 60111, Surabaya, Indonesia

² Maritime Engineering Group, Department of Civil, Maritime and Environmental Engineering, University of Southampton, United Kingdom

ARTICLE INFO

Article history:

Received 10 July 2023

Received in revised form 12 August 2023

Accepted 15 September 2023

Available online 1 January 2024

Keywords:

CFD; Crew Boat; Numerical Analysis;

Seakeeping; MSI

ABSTRACT

Seakeeping is influenced by several factors such as speed, ship hull shape, and the direction of the waves (heading angle). In this research, the crew boat is analyzed using the 3D Diffraction method to obtain the response of the ship's motion at regular waves. The study focused on analyzing the sea motion of the crew boat at different wave periods (2.58 s, 4.12 s, 5.67 s, and 7.22 s) and variation of ship speeds (0 Knot, 3 knots, 6 knots, 9 knots, 12 knots, 15 knots, and 18 knots). It used input data including the heading angle of the wave (μ) which is 180° and at a wave height of 0.5 m. The numerical analysis was carried out to determine the ship's seakeeping and compare it with NORDFORSK 1987 criteria, and also to identify the Motion Sickness Incidence (MSI) of the crews on board. Based on the results obtained, the seakeeping value of the ship accepted the criteria of NORDFORSK 1987 up to a speed of 9 knots, starting at a speed of 12 knots it does not accept the criteria. As for the operability, the comfort level of the crew while on board has an MSI index of 0% for 0 Knot, and an MSI index for 18 knots is 4.46% of the total crew of the ship namely only 1 person from 25 persons will likely feel sea sickness.

1. Introduction

Crew boats are very important in the shipping industry because they are a means of connecting onshore and offshore installations such as drilling activities, or port destinations that serve hundreds of ships at once [1]. Crew boats require only small construction or minor modifications on the platform, so this crew boat is used to move a team of workers with their equipment [2]. As one of the types of fast boats, it is necessary to pay attention to the level of comfort and safety of the passengers.

Today, ship safety is a top priority in the maritime industry [3, 4]. In general, the ship serves as a means of transportation for transporting goods or passengers. As a form of floating media, the ship will experience movement caused by internal factors due to the ship itself or external factors such as

* Corresponding author.

E-mail address: kutama@na.its.ac.id (I Ketut Aria Pria Utama)

sea waves. High sea waves accompanied by extreme and rapidly changing weather conditions can cause discomfort and may further threaten the safety of the soul at sea [5]. Therefore, in designing a ship, one aspect that needs to be considered is the safety and comfort of the crew on board. It is thus necessary to develop a ship design, such that during its operational activities it can provide optimal seakeeping so that the comfort and safety of the passengers and crew of the ship are maintained. The design of crew boats is a complex process that requires careful consideration of various factors to ensure their efficiency, safety, and performance. This article delves into the key aspects involved in the designing of crew boats, highlighting the balance between functionality and performance [6]. The effect on the comfort of the ship's crew is commonly assessed using Motion Sickness Incidence calculations (MSI) [7, 8].

Seakeeping is one of the hydrodynamic applications caused by the interaction between the fluid and the floating object [9, 10]. Ocean conditions at certain times can cause ship movements to endanger crew and passengers. Accurate prediction of the hydrodynamic behaviour of the ship's motion is very important to estimate the ship's ability to survive in hazardous conditions [11]. Motion sickness generally indicates discomfort in a moving environment, having the peak of different associated symptoms in vomiting. The response of the crew boat due to wave loads is assessed using Ansys Aqwa software. Ansys Aqwa uses the 3-dimensional radiation diffraction theory to solve the problem of seakeeping, where in this method the surface of the hull floating structures are divided into panels called a mesh [12].

Although motions and comfort has been investigated for ferries [13] and high speed passenger craft [14], the size and hull form of modern crew boats differs from these vessel types and the effect of their motions on the comfort and safety of passengers has not been investigated. In this study, the ship data used refers to the crew boat type KCT-1901. Furthermore, with the main size of the crew boat, the ship's seakeeping analysis was carried out with variations in the wave period at rest and operational conditions. The seakeeping conditions analyzed are heaving and pitching motions. The seakeeping performance of a passenger ship can be defined in terms of the average fraction of time that the actual motions and accelerations are below specified levels (habitability) [15]. An improvement in habitability will obviously improve the well-being and safety of both the passengers and crew on board. The approach taken in this research is a numerical study to determine the ship's seakeeping which is compared to the NORDFORSK 1987 criteria. The results of the study of ship movement will later be used as material for analyzing the effect on the comfort of the ship's crew by using Motion Sickness Incidence calculations (MSI) [7, 16].

2. Methodology

Numerical studies were conducted using the Computational Fluid Dynamic (CFD) method in Ansys Aqwa to determine the seakeeping of the crew boat. The main dimensions of the ship are shown in the Table 1 and the lines plan is shown in Figure 1.

Table 1
 Main dimension of crew boat

Parameter	Boat	Unit
Length Over All (LOA)	17.800	m
Length of Waterline (LWL)	16.830	m
Breadth (B)	4.500	m
Draft (T)	0.950	m
Displacement (Δ)	36.430	ton
Block Coefficient (C_B)	0.508	
Wetted Surface Area (WSA)	75.400	m ²
Longitudinal Center of Buoyancy (LCB)	6.748	m
Longitudinal Center of Floatation (LCF)	7.110	m

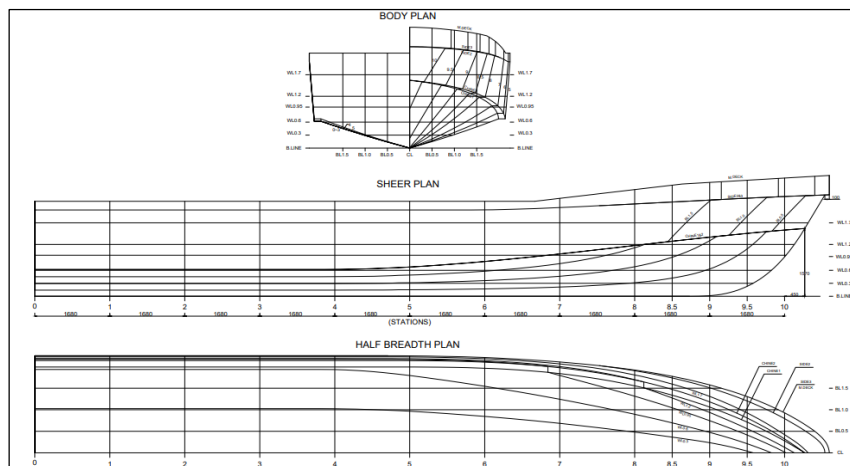


Fig. 1. Lines plan of crew boat type KCT-1901

2.1 Sea Condition

The sailing route from the crew boat is in the Senipah Harbour area, East Kalimantan as shown in Figure 2. Based on (BMKG) the height of sea waves in the operational waters of the ship is 0.5 m average in six months of 2022 [17], shown in The distance from the port to Senipah Harbour Area is about 150 miles Meteorological, Climatological and Geophysical Agency (BMKG) shown in Figure 3.

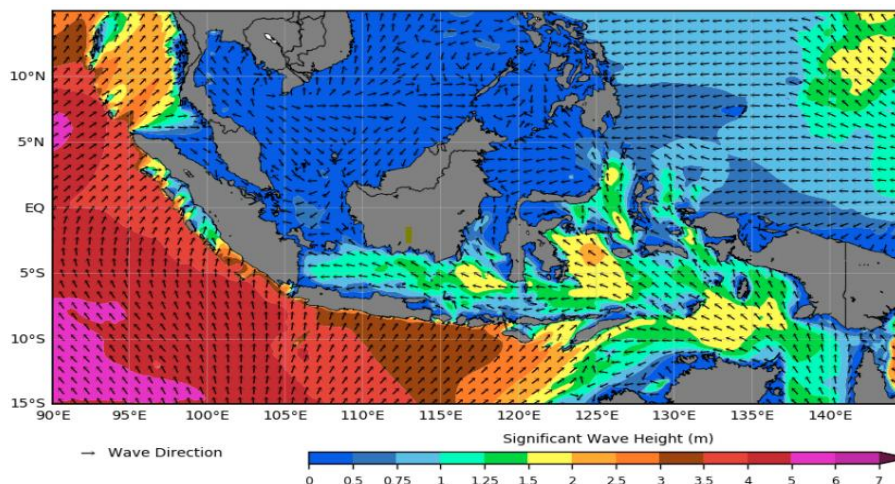


Fig. 2. Wave condition on Senipah Port area [17]

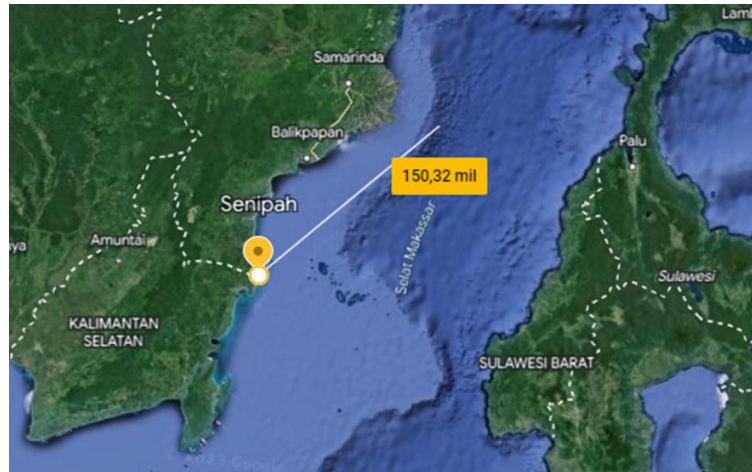


Fig. 3. Sailing distance of crew boat's [4]

2.2 Numerical Simulation

Numerical simulation is conducted using the Ansys Aqwa software. A three-dimensional (3D) model of the ship in Figure 4 is first made with Maxsurf Modeller software, then a comparison of the hydrostatic data between the 3D model and the full-scale ship is shown in Table 2. To ensure that the ship model is accurate, the index of difference in all parameters is less than 2% [13].

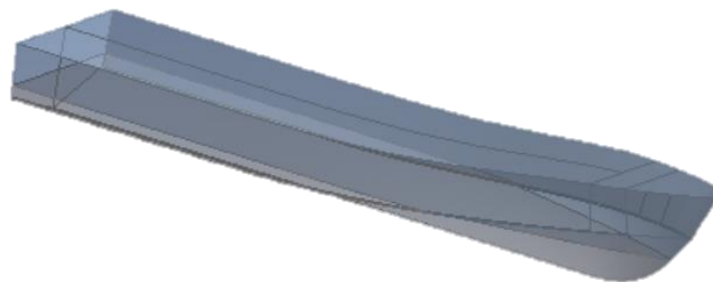


Fig. 4. 3D model of crew boat type KCT 1901

Table 2

Comparison of the hydrostatic data between the 3D model and the full-scale

Parameter	Boat	3D model	Unit	Difference (%)
Length Over All (LOA)	17.800	17.800	m	0.000
Length of Waterline (LWL)	16.830	16.808	m	0.131
Breadth (B)	4.500	4.500	m	0.000
Draft (d)	0.950	0.950	m	0.000
Displacement (Δ)	36.430	36.060	ton	1.016
Block Coefficient (C _b)	0.508	0.506		0.394
Wetted Surface Area (WSA)	75.400	75.225	m ²	0.232
Longitudinal Center of Buoyancy (LCB)	6.748	6.768	m	-0.296
Longitudinal Center of Floatation (LCF)	7.110	7.106	m	0.056

The technique used in the Ansys Aqwa software is the panel method, also known as the Boundary Element Method (BEM) [12, 18]. The panel method divides the surface of the ship into several elements. The details panel provides with options for setting up the sea geometry's Water Level, Water Depth, and size (Water Size X, Water Size Y). Figure 5 represents the computational domain with the sizes used, namely: X = 178 m (10 LOA), Y = 75.7 m (4 LOA), and Z = 53.4 m (3 LOA).

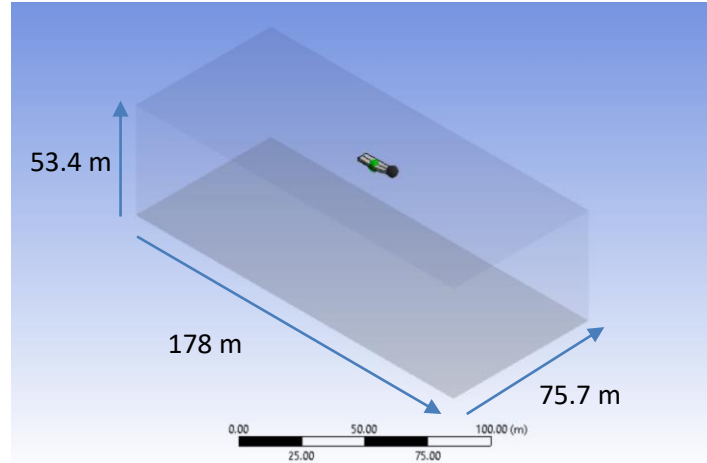


Fig. 5. Computational domain used in CFD software

Simulations were carried out to determine the motion of the ship at different operational speeds, so that several variations of the data were made as shown in Table 3. ITTC recommends [8] the radii of gyration measures as shown in Table 4.

Table 3
Variation of CFD simulation condition with Ansys Aqwa software

Parameter	Velocity (knots)						
	0	3	6	9	12	15	18
Draft (m)	0.95	0.95	0.95	0.95	0.95	0.95	0.95
Period (s)	2.58	2.58	2.58	2.58	2.58	2.58	2.58
Amplitude (m)	0.25	0.25	0.25	0.25	0.25	0.25	0.25
Heading angle (deg)	180	180	180	180	180	180	180

Table 4
Ship's Radii of Gyration

Component	Formula	Value (m)
k_{xx}	$0.34 \times B$	1.53
k_{yy}	$0.25 \times LOA$	4.45
k_{zz}	$0.25 \times LOA$	4.45

2.3 Calculation of Wave Condition

Wave conditions in Indonesian waters can be represented using the Joint North Sea Wave Project (JONSWAP) spectra [16, 19]. The JONSWAP spectra contain the parameters of the wave characteristics of closed or archipelagic waters, with the following in Eq. (1) [16, 19].

$$S_{J\zeta}(\omega_e) = 0.658CS_{B\zeta}(\omega_e) \quad (1)$$

Where the Jonswap Spectrum is denoted by $S_{J\zeta}(\omega_e)$, Bretschneider Spectrum $S_{B\zeta}(\omega_e)$, and C for coefficient factor.

For a vessel sailing with a speed (V_s) and a heading angle (μ), the encounter wave frequency (ω_e) is given in Eq. (2) [16].

$$\omega_e = \omega_w \left(1 - \frac{\omega_w V}{g} \cos \mu \right) \quad (2)$$

Where Encounter Frequency is symbolized with ω_e , wave frequency by ω_w , ship speed with V , gravitation acceleration with g , and heading angle with μ .

Furthermore, the wave spectral density as a function of the encounter wave frequency ω_e is given as follows in Eq. (3) [16].

$$S(\omega_e) = S(\omega_w) \frac{1}{1 - \left(\frac{2\omega_w V}{g}\right) \cos \mu} \quad (3)$$

Where encounter spectrum is symbolized with $S(\omega_e)$, wave spectrum with $S(\omega_w)$, wave frequency with ω_w , and encounter frequency with ω_e .

2.4 Response Amplitude Operator (RAO)

Response Amplitude Operator (RAO) is a dynamic motion function of a structure caused by waves with a certain frequency range. RAO is a tool for transferring wave force into a response to the dynamic motion of the structure in Eq. (4) [14].

$$\text{RAO}(\omega_e) = \frac{x_p(\omega_e)}{\mu_\omega(\omega_e)} \quad (4)$$

Where $x_p(\omega_e)$ is the amplitude of Motion and $\mu_\omega(\omega_e)$ is the amplitude of wave.

2.5 Calculation of Response Spectra

The calculation of the response spectrum is done by entering the Response Amplitude Operator (RAO) parameter and the wave spectrum as follows in Eq.(5) [16].

$$S_{\zeta r}(\omega_e) = [\text{RAO}(\omega_e)]^2 S_\zeta(\omega_e) \quad (5)$$

Where $S_{\zeta r}(\omega_e)$ is response spectrum, $\text{RAO}(\omega_e)$ is a transfer function, and $S_\zeta(\omega_e)$: wave spectrum its mean wave spectrum.

From the CFD test using regular waves, a bow motion will be formed. The spectral density value of the relative bow motion can be calculated by the following formula in Eq. (6) [16].

$$S_s(\omega_e) = S_z + \frac{\pi L}{L_w} S_\theta - S_\zeta \quad (6)$$

Where the symbol spectral density value of the relative bow motion is $S_s(\omega_e)$, S_z is a spectra density response spectrum for heave, S_θ is a spectra density response spectrum for pitch, S_ζ is spectra density wave spectrum, L is a distance from CG point of ship, and L_w is wave length.

Based on the spectral density value of the relative bow motion, it can be derived to obtain the vertical velocity and vertical acceleration spectra values with the following formula in Eq. (7) and Eq. (8) [16].

$$S_v(\omega_e) = \omega_e^2 S_{\zeta r}(\omega_e) \quad (7)$$

$$S_a(\omega_e) = \omega_e^4 S_{\zeta_r}(\omega_e) \quad (8)$$

Where S_v is vertical velocity and S_a is vertical acceleration as response statistics. Then, the rms and significant amplitude of the responses are calculated as a one of criteria on seakeeping based on NORDFORSK 1987. The rms value is calculated as $\sqrt{m_n}$ and the significant amplitude as $2\sqrt{m_n}$, where m_n is the area under the spectra curve.

2.6 Calculation of Slamming Probability and Deck Wetness Probability

In calculating the magnitude of bottom slamming, it must take into account the probability of the vertical motion of the bow being relatively larger than the water level at the bow ($Z_{br} > T_b$) and the probability of the relative vertical speed of the bow being greater than the threshold speed for slamming as follows in Eq. (8) [3, 16].

$$P_r(Z_{br} > T_b \text{ and } V_{br} > V_{th}) = \exp\left(-\frac{T_b^2}{2m_{0s}} - \frac{V_{br}^2}{2m_{2s}}\right) \quad (9)$$

Where the formula to Calculation of Slamming and Deck Wetness Probability is P_r , Z_{br} is a relative vertical movement of the bow V_{br} is relative velocity of bow, V_{th} is threshold velocity, T_b is bow draft, m_{0s} is a spectrum area for response relative bow motion, and m_{2s} is a spectrum area for response relative bow velocity.

In extreme weather such as hurricanes, the waves and ship motion can become so large that water can enter the deck. This problem is known as deck wetness or green water loading. The probability of deck wetness or green water is calculated as follows in Eq. (9) [3].

$$P\{s \geq f'(l)\} = e^{-f'(l)^2/2m_0} \quad (10)$$

Where The probability of deck wetness or green water can calculated by this formula $P\{s \geq f'(l)\}$, f as effective freeboard, and m_0 as area under response spectrum.

2.7 Motion Sickness Incidence (MSI)

Motion Sickness Incidence (MSI) is a standard method for estimating the discomfort and vomiting caused by various conditions of motion on ships. To determine the motion sickness experienced by passengers or crew as a result of random motion responses on board is a difficult problem [20]. This is because each individual has a different vulnerability to ship motion. The following is the MSI formula approach as a quantitative formula for the number of passengers experiencing seasickness which is expressed in percent as follows in Eq. (10) and Eq. (11) [7, 16].

$$MSI = 100 \left[0.5 + \operatorname{erf}\left(\frac{\log_{10} \frac{a_v}{g} - \mu_{MSI}}{0.4}\right) \right] \quad (11)$$

$$\mu_{MSI} = -0.819 + 2.32 \left[\log_{10} \left(\sqrt{\frac{m_4}{m_2}} \right) \right]^2 \quad (12)$$

Motion Sickness Incidence (MSI) is a standard method for estimating the discomfort and vomiting caused by various conditions of motion on ships, erf as error function, av as a average vertical acceleration one spot, μ_{MSI} as a MSI parameter, m_4 as area under curve of vertical acceleration, m_2 as an area under curve of vertical velocity.

3. Results and Discussion

3.1 Comparison between Analysis Numeric and Experiment

The validation of the results of numerical analysis with this experiment was carried out by comparing the elevation graphs of the heave movement and the ship's pitch. Experimental activities were carried out at 2 (two) variations of ship speed, namely 3 knots and 6 knots. In this experimental activity also uses several variations of the wave period including 4.12 s, 5.67 s, and 7.22 seconds.

The elevation graphs for heave motion, comparing the results from CFD simulations and experimental data, are presented in Figure 6. It can be observed that both graphs exhibit a similar trendline. However, in the experimental results, there are certain points where values cause the graph to deviate slightly, as seen at 8.13 seconds and 41.91 seconds. Between the time interval of 10 seconds to 25 seconds, both graphs closely align with each other, but beyond that, they exhibit different phases. The amplitude of heave elevation from the CFD simulation is 0.25 meters, while the experimental data yields an amplitude of 0.26 meters. Consequently, the percentage deviation resulting from the difference between these two amplitude values is 4.48%. Since the obtained deviation is less than 5%.

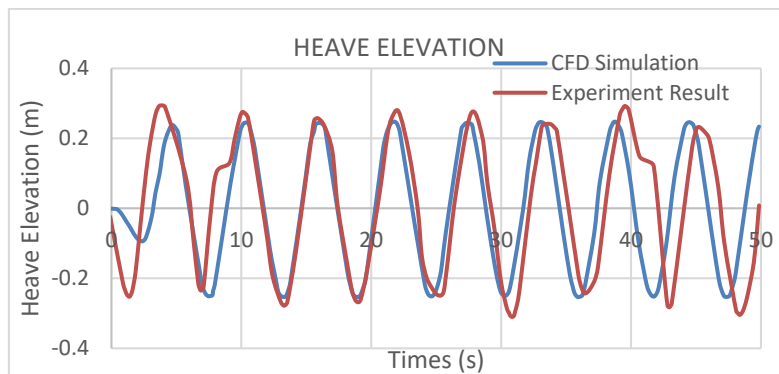


Fig. 6. Comparison heave elevation between CFD and experiment

In Figure 7, the elevation graphs for pitch motion between the CFD simulation results and experimental data are displayed. It is evident that both graphs follow the same trendline, and the experimental testing has produced consistent results without any points causing significant deviations. For the pitch elevation graph generated from the CFD simulation, the average amplitude value is 1.60 degrees. On the other hand, the pitch elevation graph obtained from the experiment has an average amplitude value of 1.75 degrees. From these two average amplitude values, it can be determined that the percentage deviation resulting from the difference between them is 8.17%. This value is relatively large, exceeding the 5%.

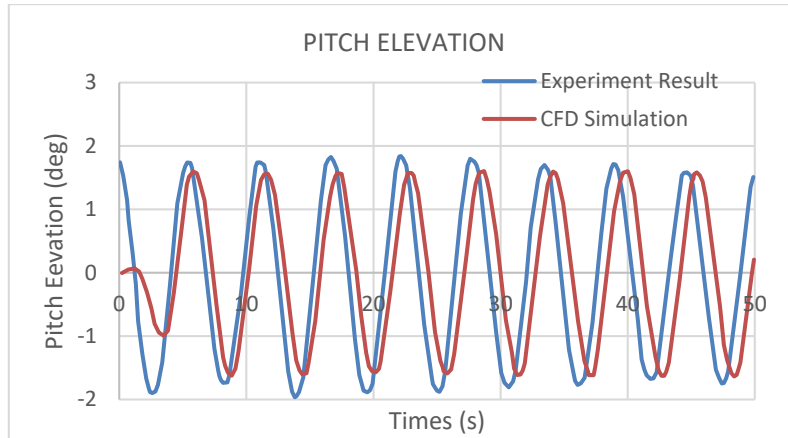


Fig. 7. Comparison heave elevation between CFD and experiment

3.2 Response Amplitude Operator (RAO)

The CFD (Computational Fluid Dynamics) software assists in analyzing seakeeping. The initial data input includes variations in speed and wave period. The obtained results include Response Amplitude Operator (RAO) graphs and graphs of heave and pitch motion elevations of the ship. The result analysis using CFD is shown in Figure 8. Figure 8a shows motion amplitude with the highest amplitude motion shows in red colour in stern area and Figure 8b shows wave surface elevation with highest value of wave amplitude shows in red colour in stern area.

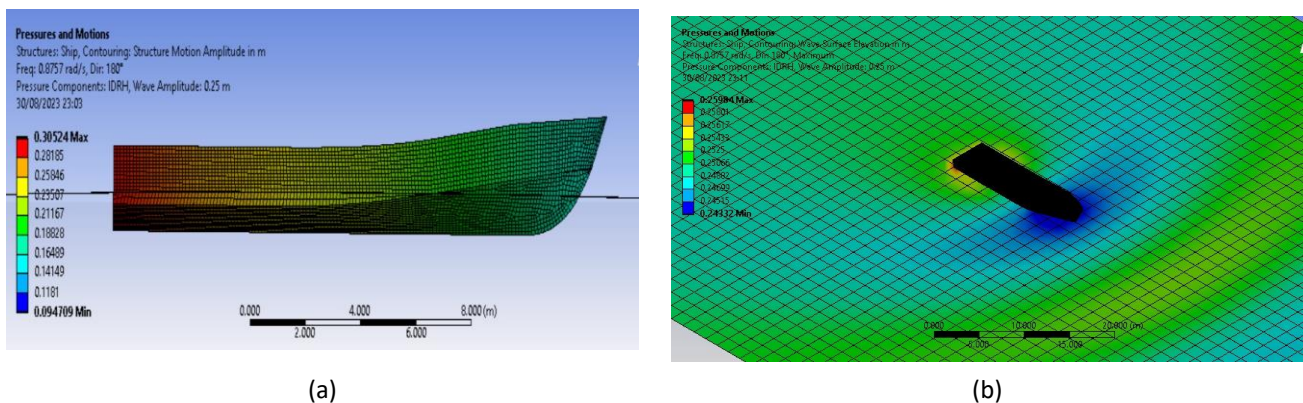


Fig. 8. Motions results in CFD (a) Motion amplitude (b) Wave surface elevation

RAO (Response Amplitude Operator) for two degrees of freedom, with heaving and pitching obtained separately [21]. In Computational Fluid Dynamics (CFD) simulations can obtain Response Amplitude Operator (RAO) data for various types of vessel motions and wave angle of 180° (head seas) and a wave height of 0.5 m (sea state 2). The waves are only coming from one direction, thus the motions are uncoupled. This analysis was carried out with variations of speed V_s , are: 0 knot, 3 knots, 6 knots, 9 knots, 12 knots, 15 knots, and 18 knots.

Figure 9 shows the RAO of the ship's heave motion. The graph shows the relationship between wave frequency and RAO in heave motion at speed variations of 0,3,6,9,12,15 and 18 knots respectively. At 0 knot speed the highest peak value is at a wave frequency of 0.05 rad/s with a RAO value of 1.000 m/m. At a speed of 3 knot the highest peak value is at a wave frequency of 0.555 rad/s with a RAO value of 1.002 m/m. At a speed of 6 knots the highest peak value is at a wave frequency of 0.692 rad/s with a RAO value of 1.035 m/m. At a speed of 9 knots the highest peak value is at a

wave frequency of 0.555 rad/s with a RAO value of 1.086 m/m. At a speed of 12 knots the peak value is at a wave frequency of 1.426 rad/s with a RAO value of 1.20 m/m. At a speed of 15 knots the peak value is at a wave frequency of 1.38 rad/s with a RAO value of 1.43 m/m. At a speed of 18 knots the peak value is at a wave frequency of 1.334 rad/s with a RAO value of 1.67 m/m. In areas with low frequencies (close to 0) the value for all speed variations is close to 1 m/m, this is because the heaving amplitude of the ship has a value that is relatively similar to the wave amplitude due to the large wavelength so that the ship moves to follow wave elevation. The graph peaks relatively increase along with the increase in ship speed [22, 23]. The highest peak occurred at a speed of 18 knots with a value of 1.671 m/m.

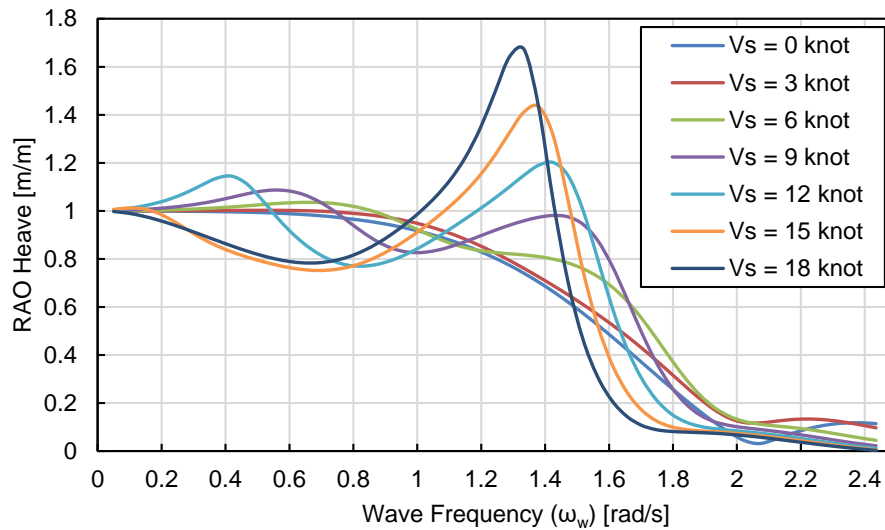


Fig. 9. Heave RAO with heading angle 180° and wave height 0.5m

Similar to the heave motion, the RAO value of the ship's pitch motion at each speeds as shown by Figure 10 has a peak value that is greater in conditions of increasing ship speed [23]. The highest peak occurred at a speed of 18 knots with a value of 20.752 °/m. At a ship speed 0,3,6,9,12,15, and 18 knots the peak point of the graph is shown at wave frequency respectively 1.655 rad/s; 1.610 rad/s; 1.610 rad/s; 1.517 rad/s, 1.472 rad/s, 1.380 rad/s, 1.334 rad/s, with the RAO value of each speeds showing successively 10.922 °/m, 13.620 °/m, 14.812 °/m, 16.200 °/m, 17.657 °/m, 19.150 °/m, and 20,752 °/m.

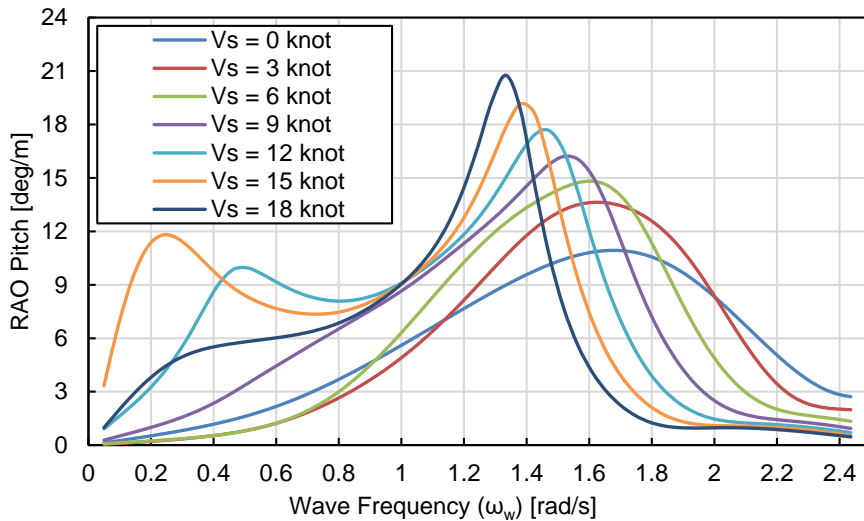


Fig. 10. Pitch RAO with heading angle 180° and wave height 0.5m

3.3 Seakeeping Analysis

The results of the response characteristics will be compared with the seakeeping criteria according to NORDFORSK, 1987 for the type of fast small craft where the criteria use the parameters of the RMS vertical acceleration value at the forward perpendicular (FP) and deck reference points, probability deck wetness, and probability slamming. The seakeeping criteria for fast small ships according to NORDFORSK, 1987 [12] can be seen in Table 5.

Table 5
 Seakeeping criteria for small fast vessel according to NORDFORSK 1987

Description	Max criteria
RMS of vertical acceleration at FP	0.65 g
RMS of vertical acceleration at Bridge	0.275 g
Probability of slamming	0.03 g
Probability of deck wetness	0.05 g

The analysis is carried out by calculating the response characteristics of the ship's motion at a wave height of 0.5 m (sea state 2) when the ship is at zero speed (0 knot) and operational conditions (3 knots, 6 knots, 9 knots, 12 knots, 15 knots and 18 knots).

Table 6 shows standard for maximum criteria according to NORDFORSK 1987 at each speed. Vertical acceleration at 0 knot until 9 knots are still acceptable by standard but 12 knots is not acceptable. Slamming will acceptable from 0 knot and 3 knots. Probability slamming only acceptable only at small speed. Probability of deck wetness is acceptable for at each speed. For all NORDFORSK criteria will acceptable at small speed

According to the analysis that has been done in Table 6 - 8, it can be concluded that the ship is only able to sail safely at a speed of 0 Knot to 9 knots. Starting at a speed of 12 knots, the ship does not meet the seakeeping criteria according to NORDFORSK, 1987 [24, 25], in particular slamming criteria are exceeded for speeds over 6 knots.

Table 6

Comparison of crew boat's seakeeping response at 0-12 knots speed with seakeeping criteria according to NORDFORSK 1987

Description	Max criteria	0 Knot	Status	3 Knot	Status	6 Knot	Status	9 Knot	Status	12 Knot	Status
RMS of vertical acceleration at FP	0.65 g	1.015	OK	2.147	OK	3.353	OK	4.575	OK	5.820	OK
RMS of vertical acceleration at bridge	0.275 g	0.740	OK	1.221	OK	1.799	OK	2.625	OK	3.483	NO
Probability of slamming	0.03 g	0.080	OK	0.197	OK	0.312	NO	0.380	NO	0.424	NO
Probability of deck wetness	0.05 g	0.000	OK	0.003	OK	0.016	OK	0.033	OK	0.048	OK

Table 7

Comparison of crew boat's seakeeping response at 15 knots speed with seakeeping criteria according to NORDFORSK 1987

Description	Max criteria	15 knot	Status
RMS of vertical acceleration at FP	6.377	7.148	NO
RMS of vertical acceleration at Bridge	2.707	3.740	NO
Probability of slamming	0.294	0.385	NO
Probability of deck wetness	0.491	0.060	OK

Table 8

Comparison of crew boat's seakeeping response at 18 knots speed with seakeeping criteria according to NORDFORSK 1987

Description	Max criteria	18 knot	Status
RMS of vertical acceleration at FP	6.377	8.521	NO
RMS of vertical acceleration at bridge	2.707	4.592	NO
Probability of slamming	0.294	0.410	NO
Probability of deck wetness	0.491	0.069	OK

3.4 Motion Sickness Incidence

The CFD (Computational Fluid Dynamics) software assists in analyzing seakeeping. The initial data input includes variations in speed and wave period. General equations from RAO use Eq. (4). CFD provides results in the amplitude of motion, the amplitude of wave added to CFD. The obtained CFD results include Response Amplitude Operator (RAO) graphs of heave and pitch motions. RAO is utilized to transform wave spectra into response spectra using Eq. (5). The response spectra can be used to determine bow motion values using Eq. (6), then vertical velocity spectra and vertical acceleration spectra can be derived using Eq. (7)-(8). This allows for the determination of the root mean square (rms) value by calculating the response moment that represents the area under the spectra curve, m_2 and m_4 are represented the area under vertical velocity spectra and vertical acceleration spectra, regarding the seakeeping criteria for the ship, where the NORDFORSK 1987 criteria are applied. This assessment aims to determine up to what speed conditions the ship can safely navigate.

Based on the seakeeping response of the ship, the Motion Sickness Incidence (MSI) is calculated using Eq. (10). This MSI formula requires several input parameters, such as μ_{MSI} , gravitational acceleration at 9.81 m/s^2 , moment of vertical velocity (m_2) and moment of vertical acceleration (m_4) of the ship. The formula also involves the correction factor for the error function, $\text{erf}(x)$. The calculation of the MSI formula as in Eq. (11) [20] requires several input parameters such as μ_{MSI} , the acceleration of gravity of 9.81 m/s^2 , and the vertical acceleration of the ship. From this formula, the error factor $\text{erf}(x)$ is also corrected. Obtained values as shown in Table 9.

Table 9
 Result of Motion Sickness Incidence (MSI) on crew

Speed (Vs) [Knot]	μ_{MSI}	Motion Sickness Incidence (MSI) [%]
0	-0.309	0.000
3	-0.583	0.000
6	-0.494	0.000
9	-0.422	0.200
12	-0.363	0.707
15	-0.328	1.756
18	-0.254	4.460

It can be seen that at a speed of 0 knot to 6 knots, it does not indicate any crew experiencing sea sickness because the MSI index shows a value of 0%. At a speed of 9 knots to 12 knots, the MSI index shows a value below 1% from 25 persons is 0.25, this shows the percentage of the number of ship crew experiencing relatively small sea sickness after 2 hours journey. And at a speed of 15 knots, the MSI index shows 1.76% of the ship's crew experiencing seasickness. And at the highest speed of 18 knots, the highest MSI index value is 4.46% from 25 persons is 0.8, this is hence only one person is likely to experience seasickness.

4. Conclusions

Based on the results of the analysis that has been carried out in CFD. CFD simulation is one of the tools that can be used to analyze the ship's RAO. Response Amplitude Operator (RAO) is a dynamic motion function of a structure caused by waves with a certain frequency range. RAO is a tool for transferring wave force into a response to the dynamic motion of the structure. CFD provides graphs of RAO for heave and pitch motions at speed variations of 0 knot to 18 knots, the highest peak values were obtained. Furthermore, sequentially for the value of the highest peak of heave motions are 1.00 m/m, 1.002 m/m, 1.035 m/m, 1.086 m/m, 1.20 m/m, 1.43 m/m, 1.67 m/m, and for pitch motions are 10.922 °/m, 13.620 °/m, 14.812 °/m, 16.200 °/m, 17.657 °/m, 19.150 °/m, and 20,752 °/m. As the velocity of the vessel increases, the peak of Response Amplitude Operator (RAO) values also exhibit a proportional increase.

The seakeeping characteristics for a ship in a stationary condition will result in maximum heaving motion when the ship is subjected to waves with a period of 7.22 seconds and a wave height of 0.5 meters, with a heading angle of 180 degrees. Meanwhile, the maximum pitching motion occurs when the ship is exposed to waves with a period of 4.12 seconds and a wave height of 0.5 meters, also at a heading angle of 180 degrees.

It was found that the ship was only able to operate up to a speed of 9 knots based on the NORDFORSK 1987 seakeeping criteria. In addition, according to the MSI formula which estimates the number of crew experiencing seasickness, it was found that at a speed of 0 knot to 6 knots there were no ship crews experiencing seasickness, but at the highest speed of 18 knots, the result of MSI

index was 4.46% of the total crew of the ship experienced seasickness, namely only 1 person from 25 persons will likely feel sea sickness.

Acknowledgement

The authors wish to thank the Institut Teknologi Sepuluh Nopember which funded the research under Outbound Research Mobility (ORM) 2023 with contract number: 153/IT.2/T/HK.00.01/2023.

References

- [1] Lamb, Thomas. 1989. *Ship Design and Construction*. Edited by Thomas Lamb. *Elements of Shipping*. The Society of Naval Architects and Marine Engineers.
- [2] El-Reedy, Mohamed A. *Offshore structures: design, construction and maintenance*. Gulf Professional Publishing, 2019.
- [3] Zhang, Xinlong, Zhuang Lin, Simone Mancini, Ping Li, Dengke Liu, Fei Liu, and Zhanwei Pang. "Numerical investigation into the effect of damage openings on ship hydrodynamics by the overset mesh technique." *Journal of Marine Science and Engineering* 8, no. 1 (2019): 11. <https://doi.org/10.3390/jmse8010011>
- [4] Supomo, Heri, and Setyo Nugroho. 2021. "Cause of Ship Accident : A Literature Review Cause of Ship Accident : A Literature Review," no. March 2021. IOP Conference Series Earth and Environmental Science. <https://doi.org/10.1088/1755-1315/557/1/012047>.
- [5] Luhulima, Richard Benny, I. K. A. P. Utama, Bagiyo Suwasono, and Sutiyo Sutiyo. "CFD Analysis into the Correlation between Resistance and Seakeeping of Trimaran Configuration." (2018). <https://doi.org/10.23977/msmi.2018.82637>
- [6] Riyadi, Soegeng, Wasis Dwi Aryawan, and I. K. A. P. Utama. "Experimental and computational fluid dynamics investigations into the effect of loading condition on resistance of hard-chine semi planning crew boat." *International Journal of Technology* 13, no. 3 (2022): 518. <https://doi.org/10.14716/ijtech.v13i3.4597>.
- [7] Gaggero, Tomaso, Filippo Bucciarelli, Giovanni Besio, Andrea Mazzino, and Diego Villa. "A method to assess safety and comfort for different ships types in a region of interest." *Ocean Engineering* 250 (2022): 110995. <https://doi.org/10.1016/j.oceaneng.2022.110995>
- [8] Scamardella, Antonio, and V. Piscopo. "Passenger ship seakeeping optimization by the Overall Motion Sickness Incidence." *Ocean Engineering* 76 (2014): 86-97. <https://doi.org/10.1016/j.oceaneng.2013.12.005>.
- [9] Tezdogan, Tahsin, Atilla Incecik, and Osman Turan. "Operability assessment of high speed passenger ships based on human comfort criteria." *Ocean Engineering* 89 (2014): 32-52. <https://doi.org/10.1016/j.oceaneng.2014.07.009>.
- [10] Waskito, Kurniawan Teguh. "On the High-Performance Hydrodynamics Design of a Trimaran Fishing Vessel." *Journal of Advanced Research in Fluid Mechanics and Thermal Sciences* 83, no. 1 (2021): 17-33. <https://doi.org/10.37934/arfmts.83.1.1733>.
- [11] Perez, Tristan. "Ship seakeeping operability, motion control, and Autonomy-A Bayesian Perspective." *IFAC-PapersOnLine* 48, no. 16 (2015): 217-222. <https://doi.org/10.1016/j.ifacol.2015.10.283>.
- [12] ANSYS Inc. 2012. "AQWA Reference Manual." *Ansys* 15317 (October): 724-46.
- [13] Riola, J. M., J. Aranda, F. Velasco, J. M. Giron-Sierra, S. Esteban, J. Recas, Toro B. Andres, and J. M. De la Cruz. "OVERVIEW OF A RESEARCH ON ACTUATORS CONTROL FOR BETTER SEAKEEPING IN FAST SHIPS." *IFAC Proceedings Volumes* 38, no. 1 (2005): 43-48. <https://doi.org/10.3182/20050703-6-cz-1902.01949>.
- [14] Fang, Chih-Chung, and Hoi-Sang Chan. "An investigation on the vertical motion sickness characteristics of a high-speed catamaran ferry." *Ocean engineering* 34, no. 14-15 (2007): 1909-1917. <https://doi.org/10.1016/j.oceaneng.2007.04.001>.
- [15] Sariöz, Kadir, and Ebru Narli. "Effect of criteria on seakeeping performance assessment." *Ocean Engineering* 32, no. 10 (2005): 1161-1173. <https://doi.org/10.1016/j.oceaneng.2004.12.006>.
- [16] Bhattacharyya, Rameswar. "Dynamics of marine vehicles." (*No Title*) (1978).
- [17] Meteorological, Climatological. "Geophysical Agency (BMKG)." *Ocean Forecast System* (2022).
- [18] Elfaghi, Abdulhafid MA, Alhadi A. Abosbaia, Munir FA Alkibir, and Abdoulhdi AB Omran. "CFD Simulation of Forced Convection Heat Transfer Enhancement in Pipe Using Al2O3/Water Nanofluid." *Journal of Advanced Research in Numerical Heat Transfer* 8, no. 1 (2022): 44-49.
- [19] Lloyd, A. R. J. M. "Seakeeping: ship behaviour in rough weather." *Admiralty Research Establishment, Haslar, Gosport, Publisher Ellis Horwood Ltd, John Wiley & Sons, ISBN: 0 7458 0230 3* (1989).

- [20] O'HANLON, James F., and Michael E. McCauley. "Motion sickness incidence as a function of the frequency and acceleration of vertical sinusoidal motion." *Aerospace medicine* 45, no. 4 (1974): 366-369. <https://doi.org/10.21236/AD0768215>
- [21] Tavakoli, Sasan, Rasul Niazmand Bilandi, Simone Mancini, Fabio De Luca, and Abbas Dashtimanesh. "Dynamic of a planing hull in regular waves: Comparison of experimental, numerical and mathematical methods." *Ocean Engineering* 217 (2020): 107959. <https://doi.org/10.1016/j.oceaneng.2020.107959>.
- [22] Im, Namkyun, and Sangmin Lee. "Effects of Forward Speed and Wave Height on the Seakeeping Performance of a Small Fishing Vessel." *Journal of Marine Science and Engineering* 10, no. 12 (2022): 1936. <https://doi.org/10.3390/jmse10121936>.
- [23] Lin, Yu-Hsien, and Chia-Wei Lin. "Numerical simulation of seakeeping performance on the preliminary design of a semi-planing craft." *Journal of Marine Science and Engineering* 7, no. 7 (2019): 199. <https://doi.org/10.3390/jmse7070199>.
- [24] DNV GL. 2015. *Finite Element Analysis*. Edited by Class guideline — DNVGL-CG-0127. Edition October 2015. Norway: DNV GL AS
- [25] Suastika, Ketut, Gilbert Ebenezer Nadapdap, Muhammad Hafiz Nurwahyu Aliffrananda, Yuda Apri Hermawan, I. Ketut Aria Pria Utama, and Wasis Dwi Aryawan. "Resistance Analysis of a Hydrofoil Supported Watercraft (Hysuwac): A Case Study." *CFD Letters* 14, no. 1 (2022): 87-98. <https://doi.org/10.37934/cfdl.14.1.8798>.